

## VELOCITY AND SHAPE SELECTION IN DENDRITIC GROWTH

Michael N. Barber

The problem of dendritic growth in solidification is formulated as a free boundary problem with an emphasis on the role of surface tension and curvature. The solvability theory of steady-state selection is described together with an analysis of time-dependent perturbations of the steady state that suggests a mechanism for side-branching due to the selective amplification of noise.

The mathematical modelling and subsequent calculation of the motion of a solidification front is the canonical example of a moving boundary problem. The motion of a particular type of solidification front—a dendritic needle crystal—is the topic of my contribution to this Conference. However, my emphasis is going to be somewhat different from that one might normally meet in discussions of solidification at a conference such as this. While some of the questions I will discuss turn out to be rather subtle mathematical questions, we will, in fact, be interested primarily in the elucidation of the physical mechanisms and parameters controlling the evolution.

I propose to begin with a brief description of the essential phenomenology of dendritic growth. We will then formulate this as a free boundary problem. However, in doing so I want to emphasise the essential physics and, in particular, the critical role that appears to be played by curvature and surface tension.<sup>1</sup> We will then turn to a particular aspect of the growth, namely the selection of the growth velocity and primary morphology. I will summarize recent work<sup>2</sup> that suggests that this selection arises mathematically through a solvability criterion that is related fundamentally to the effect of surface tension. Finally, if time permits, I would like to talk a little about the dynamics of sidebranching in dendrites, *i.e.*, the generation of the finer morphology of dendrites, in part because this is a topic to which I have contributed personally.

## Phenomenology

Imagine we supercool a fluid so that the material is still in the liquid phase but at a temperature lower than the solidification or melting temperature. Now nucleate by some mechanism (how, I am not going to worry about) a little seed of the solid. The solid will grow as the stable equilibrium thermodynamic phase. We are interested in understanding how the solid phase develops; how the solidification front propagates out into the liquid. Of course, this is a process that has many important industrial applications; its mathematical modelling and analysis has a long history and is the corner-stone of free boundary problems. However, really clean experiments designed to resolve the underlying *physical* parameters that control and determine the growth are rather more recent. The first were carried out less than twenty years ago.

Figure 1 shows the results of one of those early experiments [7]. This is a classic photograph by Fujioka (at the time a PhD student at Carnegie-Mellon University) of an ice crystal grown from very pure water under very carefully controlled experimental conditions. What emerged is somewhat similar to a snowflake but with much greater

---

<sup>1</sup>The effect of curvature and surface tension on moving boundaries seems to me, as a relative outsider, to have been rather neglected in the conventional applied mathematical literature on free boundary problems. Crank's classic book [1] mentions surface tension only once and then to state "...on neglecting surface tension".

<sup>2</sup>Much of this work has appeared in the physics literature and is perhaps not as well known to applied mathematicians working on moving boundary problems as it might be. Many of the primary sources have been reprinted recently in a review monograph, *The Dynamics of Curved Fronts*, by Pierre Pelcé [2]. For other reviews, see: Refs. [3,4,5,6].

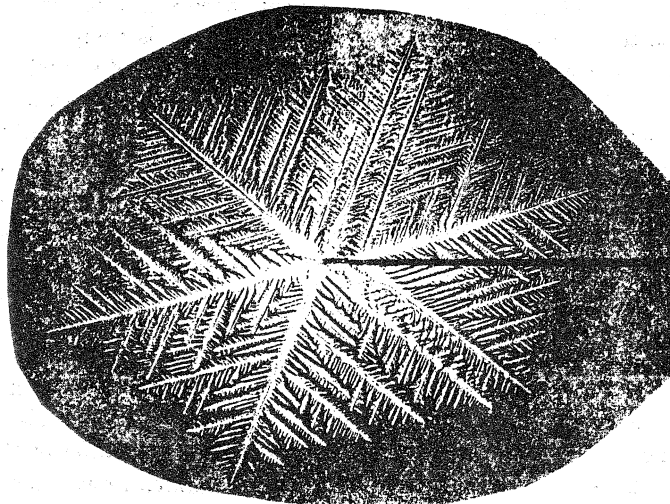


Figure 1. Photograph of dendritic ice crystal grown in pure water. (From: Ref. [7]; see, also Ref. [3]).

complexity. There is remarkable structure on several length scales—perhaps all length scales—together with considerable self-similarity. Today fractals and related ideas tend to spring immediately to mind and attempts to model dendritic crystals such as this one using fractals and fractal processes has become something of an industry.[8] However, I want to take a more classical approach and ask if there are aspects of the growth of such complex structures that can be analysed by more conventional mathematics. An answer to this question was supplied in another classic experiment, this time by Glicksman[9]. Instead of water, which has a number of experimental difficulties, Glicksman used a plastic crystal, succinonitrile, and was able to isolate the growing tip of a single dendrite, *i.e.*, one of the primary branches of the Fujioka crystal. His observations have been confirmed more recently in other systems and can be summarised with reference to Figure 2, which is a sequence of equally spaced (in time) digitized images of a growing dendrite of ammonium bromide [10].

For our purposes, the key observations are:

1. A very smooth paraboloidal tip is apparent.
2. The tip appears to grow at a uniform growth velocity since the tip moves about the same distance between each time frame.
3. Behind the tip there is a characteristic sidebranch structure, which, in time, develops its own dynamics with the tips of the sidebranches beginning to move again uniformly relative to the growing primary.

4. Ultimately, competition sets in between neighbouring sidebranches with coarsening of the surviving branches.

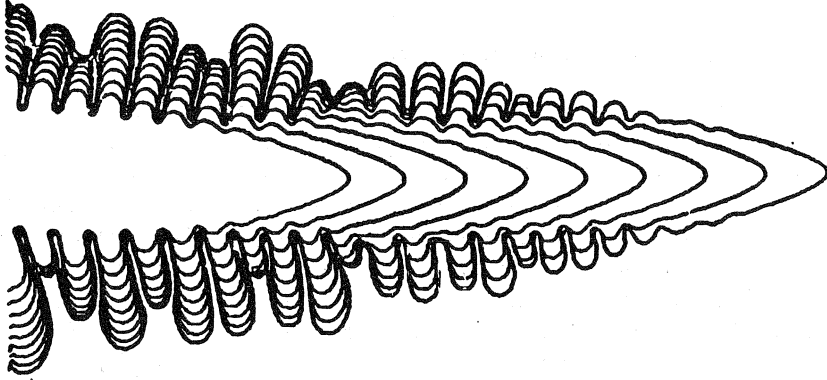


Figure 2. Contours of a growing dendrite of ammonium bromide. (From Ref. [10].)

Quantitatively, Glicksman found that the growth velocity and the tip radius were uniquely determined by the only control parameter in the problem—the degree to which he undercooled the melt.

This leads us to pose three questions at effectively three levels:

1. What selects the primary dendrite? Can we identify the processes and/or mechanisms that allow the tip radius and the growth velocity to be predicted as functions of the undercooling?
2. If we can understand that, what is the mechanism that gives rise to sidebranching? Can we predict the amplitudes, wavelengths, *etc.*, of the sidebranch structure?
3. Finally, what do we know about coarsening and the sidebranch competition that occurs further down the dendrite?

Of course, all these questions might be wrong or, perhaps better stated, the implied decoupling of the total structure might be wrong. That might be the result of some complex non-linear process. Even if that is not the case we will still need to find a way to put the sub-structures together to give the fractal structure that is apparent, for example, in Fujioka's ice crystal.<sup>3</sup>

<sup>3</sup>An example of the way this might occur is illustrated by the recent work of Eckmann and Procaccia on the somewhat related problem of diffusion-limited aggregation.[11]

However, in this lecture I will assume that we can sensibly decouple the structure and formulate what we believe today to be the simplest model that includes the essential physics of dendritic growth. On the basis of this model, we will see how far we can go in answering the first question, namely that of primary selection, and hopefully have a brief chance to look at the question of sidebranching.

### The Symmetric Model of Solidification

Our basic model known, for a reason that will become apparent shortly, as the symmetric model of solidification, is a modification of a classical model—the Stefan problem. As in the Stefan problem, the interface will be assumed to be a sharp mathematical surface separating (supercooled) liquid from (thermodynamically stable) solid. No thermodynamics or statistical mechanics enters the formulation other than the assumption that on solidification latent heat is released. Moreover, it is diffusion of this latent heat away from the front that is the rate controlling mechanism. Any other motion, for example advective motion in the liquid or dynamical effects in the solid, will be neglected. In particular, no hydrodynamics is included.<sup>4</sup> Finally we assume that material properties—diffusion constant, specific heat, *etc.*—take the same values in both phases—hence the name of the model. One can relax this assumption without too much difficulty. However, it turns out to be a pretty good approximation for succinonitrile; less so for ammonium bromide.

With these assumptions we are left with a simple equation, namely the diffusion equation

$$\frac{\partial u}{\partial t} = D\nabla^2 u, \quad (1)$$

for the temperature field, which is conveniently normalized as

$$u(\mathbf{x}, t) = \frac{T(\mathbf{x}, t) - T_\infty}{(L/c)}, \quad (2)$$

where  $T(\mathbf{x}, t)$  is the local temperature and  $T_\infty$  is the temperature far from the front. The other parameters that enter these equations are the latent heat  $L$ , the heat capacity  $c$  and the diffusion constant  $D$ , all of which are assumed to take the same values in the liquid and solid phases. Eq. (1) must now be supplemented by appropriate boundary and initial conditions. The initial value problem will not concern us and I will also be vague about the actual domain in which (1) is to be solved except to say the  $u \rightarrow 0$  at ‘infinity’. The critical boundary conditions are those applying at the moving solid/liquid front; the determination of which is part of the problem.

The first of these boundary conditions is well known, namely energy conservation across the front. This, by the standard argument, implies that the normal velocity  $v_n$  of the front is given by

$$v_n = D\mathbf{n} \cdot [(\nabla u)_{\text{solid}} - (\nabla u)_{\text{liquid}}]. \quad (3)$$

---

<sup>4</sup>For a discussion of some of the interesting effects of hydrodynamics on solidification and *vice versa*, see; *e.g.*, Ref. [12]

This boundary condition is standard; it has been mentioned before in this Conference and will undoubtedly be mentioned a lot more. Where we need to be a little bit more careful and where we depart from the classical formulation of the Stefan problem, is in the boundary condition that specifies the temperature field *at* the front. If we simply assume that

$$T_{\text{front}} = T_M, \quad (4)$$

where  $T_M$  is the melting temperature, we have, of course, the classical Stefan problem. However, this assumption neglects significant physics, namely the effect of curvature and surface tension. If we assume the front is in local thermodynamic equilibrium—conceivably also a questionable assumption—then the appropriate replacement for (4) is

$$T_{\text{front}} = T_M \left( 1 - \frac{\gamma\kappa}{L} \right), \quad (5)$$

where the correction term incorporates the so-called Gibbs-Thompson effect.[2,3] Here  $\gamma$  is the surface tension,  $\kappa$  the (principal) curvature of the surface and  $L$  is again the latent heat. Physically, this correction arises from the fact that at a *curved* front the local melting temperature is decreased if the solid phase bulges out into the liquid since it is then easier for this part of the solid to melt and is increased in the converse situation.

In terms of our scaled field variable, (5) reads

$$u_{\text{front}} = \Delta - d_0\kappa, \quad (6)$$

where

$$d_0 = \frac{\gamma c T_M}{L^2} \quad (7)$$

is a fundamental new length—the capillary length—and

$$\Delta = \frac{T_M - T_\infty}{L/c} \quad (8)$$

is the (scaled) undercooling and is the only control parameter in the problem. Clearly, we have further complicated the traditional Stefan problem. In addition to the usual difficulty of imposing a boundary condition on a surface whose determination is part of the problem, we now find that the boundary condition depends on the curvature of that (unknown) surface!

Two caveats should be mentioned at this stage. We have assumed that the solid is an isotropic, effectively a non-crystalline, material. This is, in fact, an assumption that we will need to relax ultimately by allowing the surface tension to reflect something of the crystalline anisotropy of the solid. The easiest way to incorporate this effect is to make the replacement:

$$\gamma \rightarrow \gamma(1 - \alpha f(\mathbf{n})) \quad (9)$$

in (7), where  $\mathbf{n}$  is the unit outward normal (*i.e.*, from solid to liquid) of the surface and  $\alpha$  is a simple scalar parameter measuring the strength of the anisotropy. The

function  $f$  depends on (and reflects) the crystalline nature of the solid. While this modification appears to be an essential part of the full story, I do not propose to include it explicitly in any of the mathematical details I will describe. The second assumption, which should be questioned further, is that of local thermodynamic equilibrium at the front. In the situations that apply to Glicksman's and Gollub's experiments, that is small undercoolings, this assumption is probably reasonable. On the other hand, we are dealing with a dynamic process, maybe steady state, but intrinsically non-equilibrium and there are probably kinetic corrections to (6). These have not, to my knowledge, been studied in any great detail and could in the final analysis be as important as anything else included.

The key questions at this stage are: Does this simple model, that we have defined, include the essential physics that gives rise to the structures observed in the experiment? And, if it does, can we isolate and understand the relevant selection mechanisms? Subject to the caveats I have just mentioned, the the answer to the first question appears to be yes. With regard to the second, we know that there is an instability in the problem arising from the energy balance boundary condition. In this context, this instability is known as the Mullins and Sekerka instability.[13] Physically, the instability arises from the fact, explicit in (3), that the normal velocity of the front is proportional to the gradient of the temperature. Hence, if the solid bows out into liquid the level surfaces of the temperature field in the liquid will be compressed thereby sharpening the gradient in the liquid and consequently increasing the local growth velocity of the bump which becomes sharper which accentuates the whole process. Mathematically, it is straightforward to carry out [13,3] a proper stability analysis that confirms this heuristic picture. Physically, of course, perturbations of the front do not grow indefinitely because of surface tension which resists bending of the interface. Presumably the resultant patterns we see in dendritic growth are the result of a delicate balance between the morphological Mullins/Sekerka instability and this stabilisation by surface tension.

## Needle Crystals

Let us now sharpen our questions and ask about the sort of solutions we would like to find. To do so it is worthwhile, as in any good applied mathematics, to get the scales right and non-dimensionalise appropriately. We are interested in what we will call needle crystal solutions; hopefully, they will look something like the tip of one of Glicksman's or Gollub's dendrites. In fact, it is convenient to set our scales by reference to the tip radius  $\rho$  and the growth velocity  $v$ . Two dimensionless numbers are relevant:

$$p = \frac{v\rho}{2D} = \frac{\rho}{\ell_D}, \quad \sigma = \frac{d_0}{\rho p}. \quad (10)$$

The first is the *Péclet number*, which is the ratio of the tip radius to the diffusion length associated with the diffusion field. The other parameter involves the the capillary length and hence surface tension. These will be our main parameters; clearly if  $p$

and  $\sigma$  are known we can infer  $v$  and  $\rho$ . Experimentally,  $p$  and  $\sigma$  are expected to be uniquely determined by the only control parameter, the undercooling  $\Delta$ .

In Glicksman's experiments on succinonitrile,  $\Delta$  ranged from something like 0.003 to about 0.06. For this range of undercooling the Péclet number was between about  $10^{-4}$  and  $10^{-2}$  while  $\sigma$  was about 0.02 and essentially independent of  $\Delta$ . The important point to reemphasise is that, given  $\Delta$ , unique values of  $\rho$  and  $v$  and hence unique values of the Péclet number and the parameter  $\sigma$  appear to exist. Mathematically the question is: Does the symmetric model sustain steady needle crystals growing with a unique velocity and a unique tip radius?

### Equation of Motion for the Interface

The free boundary problem defined above can be reformulated as an explicit equation of motion for the interface.<sup>5</sup> To do so it is convenient to go to a frame moving with the tip velocity  $v$  of the dendrite and measure lengths in units of the tip radius  $\rho$  and time in terms of  $\rho/v$ . In this comoving frame, we anticipate that solutions will be similar to Glicksman's needle crystals and that the interface itself can be mathematically described by a graph, for example

$$z = \zeta(x, t) \quad (11)$$

in two dimensions. (We assume that the direction of motion is in the positive  $z$ -direction.)

The great mathematical simplification that ensues from the assumptions that underlie the symmetric model is that this interface acts simply as a (line or surface) source for the diffusion equation. Hence solving the diffusion equation by a Green's function, we can write down an explicit equation of motion for the front. In two dimensions this reads:

$$\begin{aligned} \Delta - \frac{d_0}{\rho} \kappa[\zeta(x, t)] &= p \int_0^\infty \frac{d\tau}{2\pi\tau} \int_{-\infty}^\infty dx' [1 + \dot{\zeta}(x', t - \tau)] \\ &\times \exp\left(-\frac{p}{2\tau} \left\{ (x - x')^2 + [\zeta(x, t) - \zeta(x', t - \tau) + \tau]^2 \right\}\right), \end{aligned} \quad (12)$$

where  $\dot{\zeta} = \partial\zeta/\partial t$  and

$$\kappa[\zeta] = \frac{-\partial^2\zeta/\partial x^2}{[1 + (\partial\zeta/\partial x)^2]^{3/2}} \quad (13)$$

is the curvature. The equation in three dimensions is similar. However, for simplicity I will restrict attention to two dimensions since there appears to be little significant difference between two and three dimensions.[16]

Physically, the left-hand side of (13) is the local temperature along the solidification front, while the right-hand side is the same temperature obtained directly by

---

<sup>5</sup>In the physics or metallurgical literature this equation appears to have been first derived by Nash and Glicksman[14]; a simple derivation is given in Ref. [3]. A more precise and more general derivation has been given recently by Strain[15].

solving the diffusion equation with the front acting simply as a line source of differential strength  $(1 + \dot{\zeta})dx$ ; the kernel being the Green's function for two-dimensional diffusion. This equation appears to be such a complicated integro-differential equation that any chance of significant numerical let alone analytical progress would seem unlikely. In the remainder of this lecture I want to show you that it is possible to explore the nature of the solutions in some detail *analytically* and thereby elucidate a number of physical consequences.

### Steady-state Solutions

Let us go then to the steady state. Remember we are working in a frame that is moving at the (assumed) steady-state velocity. Hence in the steady state, we have  $\zeta(x, t) = \zeta(x)$  and we can simply drop the explicit time dependence in (13). Evaluating the integral over  $\tau$  reduces (13) to

$$\Delta + \frac{\sigma p \zeta''(x)}{[1 + (\zeta'(x))^2]^{3/2}} = \frac{p}{\pi} \int_{-\infty}^{\infty} dx' e^{-p[\zeta(x) - \zeta(x')]} \times K_0 \left[ p \sqrt{(x - x')^2 + (\zeta(x) - \zeta(x'))^2} \right], \quad (14)$$

where  $K_0$  is the modified Bessel function. Since  $K_0(z) \sim \ln z$  for small  $z$ , the integral operator in (14) is singular. More importantly, (14) also involves a singular differential operator since  $\sigma$  multiplies the highest order derivative. A number of questions immediately arise. Do solutions exist? How many of them are there? Do they have the properties—smoothness, regularity, *etc*—that we expect physically? Are they stable? What happens to perturbations? These questions will be the focus of the rest of my talk.

### The Ivantsov Parabolas

If we neglect surface tension, that is set  $\sigma = 0$  in (14), we can write down explicit solutions provided the undercooling and Péclet number are related by

$$\Delta = 2e^p \sqrt{p} \int_{\sqrt{p}}^{\infty} e^{-y^2} dy \sim \sqrt{\pi p}, \quad p \rightarrow 0. \quad (15)$$

These solutions are the famous Ivantsov parabolas<sup>6</sup>

$$\zeta(x) = -\frac{1}{2}x^2, \quad (16)$$

first obtained in the 1940's by Ivantsov[18] directly from the diffusion equation.<sup>7</sup>

<sup>6</sup>In three dimensions, the corresponding solutions are paraboloidal cylinders and (15) is replaced by  $\Delta = pe^p \int_p^{\infty} dy e^{-y}/y \sim -p \ln p$ . Solutions with elliptical cross-sections also exist.[17]

<sup>7</sup>In the context of the Nash-Glicksman integral equation the neatest direct derivation of the Ivantsov solutions is that given by Pélce and Pomeau.[19]

Since we are using the tip radius as our length scale, (16) and (15) define a *one-parameter* family of steady-state solutions travelling in the positive  $z$  direction. The tips are certainly parabolic (paraboloidal in three dimensions). However, we have no velocity selection; only the product  $\rho v$  being determined by (15). Thus our question has now become: How does this one-parameter family break down (if it does at all) to give the apparently unique solution suggested experimentally?

Given the way that I have formulated the problem a possible answer is rather obvious. As I have already mentioned,  $\sigma$  multiplies the highest order derivative in (14). Hence neglecting surface tension is a very singular perturbation of (14). Rather surprisingly, this does not seem to have been realized until the early 1980's and the advent of some simpler models—the geometrical and boundary layer models—in which the non-locality of the diffusion field was neglected. These models were analytically tractable and the singular role of the surface tension manifest.<sup>8</sup>

### Solvability

While the detailed mathematical analysis of the effect of surface tension on the Ivantsov parabolas is rather technical, I would like to give a flavour of it for two reasons. Firstly, because it is a rather nice example of a classical technique—the WKB approximation—being adapted to a very non-trivial nonlinear problem and secondly because there are a number of open mathematical questions that need to be cleaned up before the story is complete.

Partly for personal reasons and partly because it seems intrinsically simpler, I propose to describe the approach of Langer and his group at Santa Barbara [16]. Related ideas have been developed by Kessler, Koplik and Levine [23], then with Schlumberger-Doll in Connecticut, and by Pélce, Pomeau and coworkers [19] in Paris. Mathematically, the most elegant and most nearly rigorous discussion is that of the French group, which is based on unpublished ideas of Kruskal and Segur. The weakness of the Langer approach is an unsystematic linearization at the beginning of the calculation. The French group avoids this by a method that can be described as “matched asymptotics in the complex plane”. However, the results of both approaches appear to be essentially identical.

Let us rewrite (14) as

$$\Delta - p\sigma\kappa[\zeta] = p\Gamma(\zeta, x; p), \quad (17)$$

where

$$\Gamma(\zeta, x; p) = \frac{1}{\pi} \int_{-\infty}^{\infty} dx' e^{-p[\zeta(x) - \zeta(x')]} K_0 \left[ p\sqrt{(x - x')^2 + (\zeta(x) - \zeta(x'))^2} \right] \quad (18)$$

---

<sup>8</sup>These models were introduced simultaneously in 1983—the geometrical model by the Schlumberger group [20] and the boundary layer model by Langer and co-workers [21] at Santa Barbara. Subsequent work is cited and reviewed in Refs. [2,4,5]. See, also: [22], where more rigorous discussions—with an emphasis on the singular nature—of the basic mathematical equation are presented.

and

$$\kappa[\zeta] = \frac{-\zeta''(x)}{[1 + (\zeta'(x))^2]^{3/2}}. \quad (19)$$

The Ivansov condition (15) can be expressed as

$$\Delta = p\Gamma(-\frac{1}{2}x^2, x; p). \quad (20)$$

Now subtract this result from (17), linearize<sup>9</sup> about the Ivantsov solution by writing

$$\zeta(x) = -\frac{1}{2}x^2 + \zeta_1(x) \quad (21)$$

and take<sup>10</sup> the limit  $p \rightarrow 0$ . The result is a *linear* integro-differential equation for  $\zeta_1(x)$ . For our current discussion only the essential structure of this equation is needed. To expose this structure it is convenient to set

$$\zeta_1(x) = (1 + x^2)^{3/4}Z(x). \quad (22)$$

Then on omitting some non-singular terms of  $O(\sigma)$ , the equation for  $Z$  can be written as[16]

$$(\mathcal{D}_2 + \mathcal{A})Z = \frac{\sigma}{(1 + x^2)^{3/4}}, \quad (23)$$

where

$$\mathcal{D}_2 = \sigma \frac{d^2}{dx^2} + (1 + x^2)^{1/2} \quad (24)$$

is a self-adjoint differential operator and

$$\mathcal{A}Z(x) = \mathcal{P} \int_{-\infty}^{\infty} \frac{\eta(x, x')}{x - x'} Z(x') dx' \quad (25)$$

is a singular integral operator ( $\mathcal{P}$  denoting a Cauchy principal value). The only facts we need concerning the kernel  $\eta(x, x')$  are that it is not anti-symmetric, so that  $\mathcal{A}$  is not self-adjoint, and  $\eta(x, x) \neq 0$ .

Eq. (23) is an inhomogeneous linear operator equation and hence a necessary condition for a solution to exist is that the inhomogeneous term must be orthogonal to the null space of the adjoint of  $\mathcal{D}_2 + \mathcal{A}$ . Explicitly, we require

$$\Lambda(\sigma) = \int_{-\infty}^{\infty} \frac{\tilde{Z}_H(x)}{(1 + x^2)^{3/4}} dx = 0, \quad (26)$$

---

<sup>9</sup>This somewhat premature linearization is the step that is avoided by the analysis of Pélce and Pomeau.[19]

<sup>10</sup>This step is not as extreme as it appears. What we are about to obtain is the leading order behaviour of  $\zeta_1(x)$  for small  $\sigma$ . Thus it will transpire that what we actually require is  $p \ll \sqrt{\sigma}$ , which is certainly valid experimentally; recall that for succinonitrile  $10^{-4} < p < 10^{-2}$ , while  $\sqrt{\sigma} \sim 0.14$ . In any case, the analysis can be carried through for finite  $p$  with apparently no qualitative differences.[24,25]

where

$$(\mathcal{D}_2 + \mathcal{A}^\dagger) \tilde{Z}_H = 0 \quad (27)$$

with

$$\mathcal{A}^\dagger \tilde{Z} = -\mathcal{P} \int_{-\infty}^{\infty} \frac{\eta(x', x)}{x - x'} \tilde{Z}(x') dx'. \quad (28)$$

Eq. (26) is our desired solvability condition and reduces the question of the existence of steady-state solutions to one of the existence of zeros of  $\Lambda(\sigma)$ . At this point, it turns out that significant progress can be made if we assume that

$$\tilde{Z}_H(x) \approx e^{W(x)/\sqrt{\sigma}}, \quad \text{as } \sigma \rightarrow 0, \quad (29)$$

where

$$W(x) = W_0(x) + \sqrt{\sigma}W_1(x) + O(\sigma). \quad (30)$$

The ansatz (29) will be recognized as a simple WKB approximation, which is a standard approach to singular ordinary differential equations. This is reflected in the action of  $\mathcal{D}_2$ :

$$\mathcal{D}_2 \tilde{Z}_H(x) = \{[W_0'(x)]^2 + (1 + x^2)^{1/2}\} e^{W_0(x)/\sqrt{\sigma}} + O(\sqrt{\sigma}). \quad (31)$$

Turning to the action of  $\mathcal{A}^\dagger$  we obtain

$$\mathcal{A}^\dagger \tilde{Z}_H(x) \approx -\mathcal{P} \int_{-\infty}^{\infty} \frac{\eta(x', x)}{x - x'} e^{W(x')/\sqrt{\sigma}} dx', \quad (32)$$

where the integral can be evaluated for small  $\sigma$  by the method of steepest descents. Points of stationary phase turn out to occur at  $x = \pm i$  with  $\text{Re} W(\pm i) < 0$  so that the dominant contribution to the integral arises from the pole at  $x' = x$ . Hence

$$\mathcal{A}^\dagger \tilde{Z}_H^\pm \approx \mp i\pi\eta(x, x) e^{W_0^\pm(x)/\sqrt{\sigma}}. \quad (33)$$

Combining this expression with (31) yields, to leading order in  $\sqrt{\sigma}$ , ordinary differential equations for  $W_0^\pm$ . The choice of sign in (33) reflects the choice of closing the contour in (32) in the the upper or lower  $x'$ -plane, respectively. Both choices are acceptable and lead to the two linearly independent solutions of (27). Requiring  $\tilde{Z}_H(x)$  to be real implies that the appropriate combination as far as the solvability condition (26) is concerned is equivalent to taking  $\tilde{Z}_H(x) = 2\text{Re}\{\exp(W_0^+(x)/\sqrt{\sigma})\}$ . It is then a straightforward calculation to show that

$$\Lambda(\sigma) \sim N\sigma^{-1/28} e^{-\bar{a}/\sqrt{\sigma}}, \quad \sigma \rightarrow 0, \quad (34)$$

where  $N$  and  $\bar{a}$  are positive constants. Recalling that the solvability condition reads  $\Lambda = 0$  we are left with the conclusion that there are no steady-state solutions for small  $\sigma$ ; the whole Ivantsov family has been destroyed!

This analysis is, of course, restricted to the limit  $\sigma \rightarrow 0$  and it is conceivable that solutions exist for larger values of  $\sigma$ . To investigate this regime it is necessary to turn to numerical calculations. These are facilitated if the solvability condition is

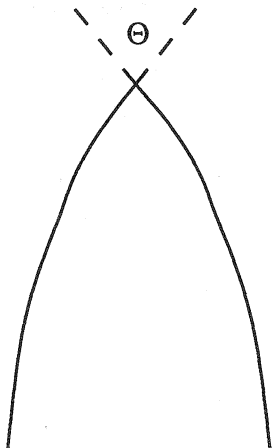


Figure 3. Cusped dendrite.

reinterpreted in a particularly illuminating way. Since we are interested in axially-symmetric solutions, we can reformulate (14) as an equation on  $0 \leq x < \infty$ , with the boundary condition

$$\zeta'(0) = 0 \quad (35)$$

at  $x = 0$  so that the tip is smooth. It is now natural to relax this condition and allow a cusp at the tip. If we denote the (outer) angle of the cusp by  $\Theta$  (see Fig. 3), one can show that the solvability criterion now reads:

$$\Lambda(\sigma) \propto (\pi - \Theta) \quad (36)$$

so that given (34) a solution exists for finite  $\sigma$ . This interpretation of the solvability criterion—namely, smoothness at the tip—has been confirmed in numerical calculations[23,26]. Admittedly, since  $\Lambda(\sigma) \sim e^{-a/\sqrt{\sigma}}$ , numerical calculations for small  $\sigma$  are subtle and care must be exercised over questions such as grid spacing to ensure that spurious solutions are not generated. Nevertheless, the absence of smooth steady-state needle crystals in the symmetric model with non-zero  $\sigma$  appears to be confirmed rather convincingly.

### Anisotropic Surface Tension

Clearly, if we accept this conclusion something has to be added to our basic model if it is to yield steady-state needle crystals; assuming, of course, that the experimental observations correspond to mathematical steady-state solutions. The conventional assumption today is that the additional ingredient is anisotropy in the surface tension reflecting the crystalline nature of the solid phase.

In one sense crystalline anisotropy is a crucial determinant of the morphologies seen in solidification—snowflakes, for example, owe their characteristic six-cornered

shapes to the underlying hexagonal symmetry of ice. Whether its role in steady-state selection is equally critical is somewhat less clear.

Mathematically, the simplest way to include the effects of crystalline anisotropy on the surface tension is to specify the function  $f(\mathbf{n})$  in (9), where  $\mathbf{n}$  is the outward normal to the solid surface. A realistic specification of  $f$  involves a detailed knowledge of the surface structure with precise *quantitative* conclusions likely to depend on the fine details.<sup>11</sup> In two dimensions the situation is simpler since it suffices to assume that  $f$  is simply a function of the angle  $\theta$  between the normal and the  $z$ -axis, *i.e.* the direction of growth. If we then assume say four-fold symmetry for the crystalline phase a suitable definition of  $f$  is

$$f(\theta) = \cos 4\theta. \quad (37)$$

With this choice it is possible to redo the solvability analysis described earlier with the conclusion that the solvability function  $\Lambda(\sigma; \alpha)$  now exhibits a solution  $\sigma^*$ , which is, of course, a function of the anisotropy strength  $\alpha$ . For small  $\alpha$

$$\sigma^* \sim \alpha^{7/4} \quad (38)$$

with linear behaviour for larger values.[16,25]

### Experimental Evidence for Solvability

These predictions for the variation of the observed value of the parameter  $\sigma$  with anisotropy suggests that a detailed experimental test of solvability might be possible. Unfortunately, the situation is rather more complicated for a number of reasons. On one hand, as already mentioned, an accurate determination of  $\sigma$  is likely to require a rather detailed knowledge of surface structure. On the other hand, the range of experimentally suitable materials is not extensive. Those experiments to date which are accurate enough to be contenders for a detailed test of the solvability theory do not show a great deal of variation in anisotropy. What experimental evidence is available suggests that the variation of  $\sigma$  with anisotropy is rather less than predicted theoretically. Certainly there is no evidence for as strong a variation as in (38) but as Langer [6] has discussed recently this limit is unlikely to be achievable experimentally.

To date, the most detailed and careful attempt to compare the predictions of the solvability theory with experiments is that made by Barbieri and Langer[25]. Using direct experimental estimates of the anisotropy strength for succinonitrile and ammonium bromide, Barbieri and Langer calculated the values  $\sigma^*$  predicted by solvability and compared these with the experimentally observed values  $\sigma_{\text{expt}}$ . For succinonitrile agreement was not particularly good: solvability predicting  $\sigma^* \approx 0.0092$  compared to a value of  $\sigma_{\text{expt}} \approx 0.0195$  reported by Glicksman. For Gollub's experiments on super-

---

<sup>11</sup>For attempts to construct physically reasonable yet mathematically tractable models of the surface energy, see: [25,27]

saturated ammonium bromide<sup>12</sup> rather better agreement was found with  $\sigma^* \approx 0.083$  and  $\sigma_{\text{expt}} \approx 0.081$ . Whether this agreement is fortuitous or the disparity in the case of succinonitrile is due to errors in the modelling of anisotropy is unclear at this stage. Further experiments and better three dimensional calculations remain desirable.

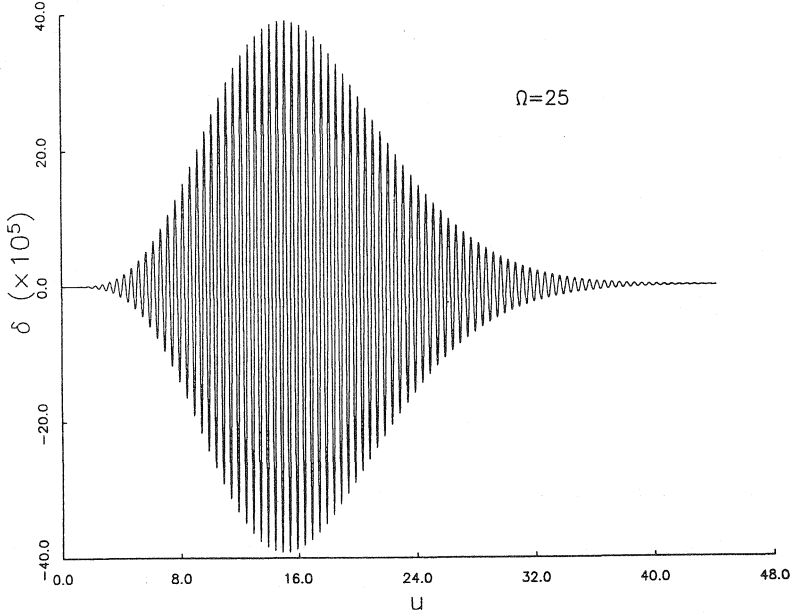


Figure 4. Normal displacement  $\delta$  of a steady-state needle crystal to a fixed frequency perturbation of frequency  $\Omega = \omega/p\sqrt{\sigma}$  with  $p = 0.08$  and  $\sqrt{\sigma} = 0.13$ . Note that the abscissae are in units of the diffusion length  $\ell = 2D/v$ . (From:Ref. [28].)

### Sidebranching

Let me now leave the question of the selection of the primary dendrite and give a brief discussion of a possible mechanism for the generation of the secondary morphology—sidebranching. We begin with a consideration[28] of the response of the steady-state solution—assumed to be an Ivantsov parabola corresponding to the value of  $\sigma$  predicted by solvability—to a fixed frequency perturbation applied to the tip. This response can be calculated[28] analytically by substituting

$$\zeta(x, t) = -\frac{1}{2}x^2 + \hat{\zeta}_1(x, \omega)e^{i\omega t/\sqrt{\sigma}} \quad (39)$$

<sup>12</sup>Technically, solvability theory for  $\text{NH}_4\text{Br}$  needs to be extended to the non-symmetric case, *i.e.*, different diffusion constants in the two phases; indeed,  $\text{NH}_4\text{Br}$  appears to be well modeled by the one-sided model, in which no diffusion occurs in the solid phase.

into (13) and expanding to first order in  $\hat{\zeta}_1$ . The resulting equation has a similar structure to that analysed in the steady-state case. An explicit expression for  $\hat{\zeta}_1(x, \omega)$  can be obtained by similarly assuming a WKB form for  $\hat{\zeta}_1$ .

The resulting deformation of the steady-state needle-crystal is illustrated in Figure 4, which depicts the normal displacement from the steady-state interface as a function of arc-length down the dendrite.<sup>13</sup> The most notable feature is a dramatic amplification (by a factor of over  $10^6$ ) within a distance down the dendrite of a few tip radii. The distance at which the response is maximum increases as the frequency decreases. One should be cautious in the physical interpretation of these results since they are based on a linear analysis. There are undoubtedly non-linear effects. For example, we know of modes that travel up the dendrite, so that non-linear feedback mechanisms could modify the behaviour evident in Figure 4 significantly.

Let us set that issue to one side and ask if this selective amplification could be relevant to the generation of the observed sidebranch structures. Physically, we would expect spatially localised perturbations to be more relevant than a fixed frequency perturbation. We can, of course, build such a perturbation by forming a wave packet:

$$\zeta_1(x, t) = \int_{-\infty}^{\infty} A(\omega) \hat{\zeta}_1(x, \omega) e^{i\omega t / \sqrt{\sigma}} d\omega, \quad (40)$$

where  $A(\omega)$  is some suitably smooth (and broad) function. For small  $\sigma$ , the dynamics of the wave packet can be determined[28] by replacing  $\hat{\zeta}_1$  with its WKB estimate and then estimating the integral by a saddle point approximation. The resulting behaviour is distinctly different from that of a single frequency perturbation and, from the point of view of sidebranching, rather suggestive. Instead of ultimately decaying, the packet continues to grow exponentially. This growth is a direct consequence of the assumption that the initial pulse contains arbitrarily small frequencies, which it will if the initial pulse is spatially localised. If we define

$$\bar{z} = \frac{1}{2}x^2, \quad (41)$$

which is essentially the distance down the vertical axis of the dendrite, we find[28] that the amplitude of the packet grows as

$$\exp(a\bar{z}^{1/4}/\sqrt{\sigma}), \quad (42)$$

where  $a$  is a constant. The centre of the pulse moves so that  $\bar{z}_c \sim t$ . Hence the pulse actually remains stationary in the laboratory frame with the (unperturbed) tip growing away from it in the positive  $z$ -direction. (Recall we are working in a coordinate system that is comoving with the tip.)

Is this a possible mechanism for the genesis of sidebranches? An obvious source of the initial perturbation is thermal noise.<sup>14</sup> One can in fact estimate [31] by how much

<sup>13</sup>The distance parameter  $u$  is defined[28] by  $u = \frac{1}{2}p [(1 + 2x^2)^2 - 1]^{1/2}$  and is such that  $u \simeq s$  for  $x \ll 1$  and  $u \simeq 2s$  for  $x \gg 1$ , where  $s$  is the arc length.

<sup>14</sup>The possibility that sidebranches could be the result of selective amplification of thermal noise was first put forward by Pieters and Langer[29] on the basis of calculations on the local boundary-layer model. For a related discussion, see: Ref. [30].

and on what scale thermal noise would be magnified by this selective amplification. Unfortunately, it appears that thermal noise is probably an order of magnitude too small to give rise to sidebranches on the scales observed experimentally. On the other hand, all of the theoretical calculations to date are based on linear calculations and the neglected nonlinearities could easily enhance the amplification. Indeed, there is a recent experimental evidence[32] that suggests that the selective noise amplification could be correct. In this experiment, a laser was used to create a brief localized heat pulse near the smooth tip of a growing dendrite of succinonitrile—precisely, as envisaged in the theoretical calculation. Initially, the induced deformation was unobservably small but grew rapidly into a sidebranch-like feature. Indeed, preliminary analysis of the rate of growth the amplitude was not inconsistent with the theoretical prediction (42). While it would be premature to draw firm conclusions from this comparison between theory and experiment, the experimental results are encouraging and very suggestive.

It is certainly the case that tips of growing dendrites are intriguing dynamical systems that are exquisitely sensitive to small perturbations. The role that sensitivity plays in the emergence of the full morphology is a story that is yet, I think, to be completely resolved. Currently there are probably more questions than answers. It is likely that when all of these answers are in, dendritic growth will have proven to be a particularly rich and fascinating chapter in the history of moving boundary problems.

## References

1. J. Crank, *Free and Moving Boundary Problems*, Clarendon, 1984.
2. P. Pelcé, *Dynamics of Curved Fronts*, Academic Press, 1989.
3. J. S. Langer, "Instabilities and pattern formation in crystal growth", *Rev. Mod. Phys.* **52** (1980) 1-28.
4. J. S. Langer, "Lectures in the theory of pattern formation" in *Chance and Matter* (Les Houches XLVI 1986), Elsevier, 1987.
5. D. A. Kessler, J. Koplik and H. Levine, "Pattern selection in fingered growth phenomena", *Adv. Phys.* **37** (1988) 255-339.
6. J. S. Langer, "Dendrites, viscous fingers and the theory of pattern formation", *Science* **243** (1989) 1150-1156.
7. T. Fujioka, Ph.D. Thesis, Carnegie-Mellon University, 1978; see, also, Ref. [3].
8. See: *e.g.*, *Random Fluctuations and Pattern Growth*, H. E. Stanley and N. Ostrowsky (editors), Kluwer Academic, 1988.
9. S.-C. Huang and M. E. Glicksman, "Fundamentals of dendritic solidification—I. Steady-state tip growth", *Acta Metall.* **29** (1981) 701-715; "II. Development of sidebranch structure", *Acta Metall.* **29** (1981) 717-734.
10. A. Dougherty, P. D. Kaplan and J. P. Gollub, "Development of sidebranching in dendritic crystal growth", *Phys. Rev. Lett.* **58** (1987) 1652-1655; A. Dougherty and J. P. Gollub, "Steady-state dendritic growth of  $\text{NH}_4\text{Br}$  from solution", *Phys. Rev. A* **38** (1988) 3043-3053.

11. J.-P. Eckmann, P. Meakin, I. Procaccia and R. Zeitak, "Growth and form of noise-reduced diffusion-limited aggregation", *Phys. Rev. A* **39** (1989) 3185-3195.
12. R. C. Kerr, M. G. Worster, A. W. Woods and H. E. Huppert, "Disequilibrium and macrosegregation during solidification of a binary melt", *Nature* **340** (1989) 357-362.
13. W. W. Mullins and R. F. Sekerka, "Stability of a planar interface during solidification of a dilute binary alloy", *J. Appl. Phys.* **3** (1964) 444-451.
14. G. E. Nash and M. E. Glicksman, "Capillarity-limited steady-state dendritic growth—I. Theoretical development." *Acta Metall.* **22** (1974) 1283-1299.
15. J. Strain, "A boundary integral approach to unstable solidification", *J. Comp. Phys.* **85** (1989) 342-389.
16. A. Barbieri, D. C. Hong and J. S. Langer, "Velocity selection in the symmetric model of dendritic crystal growth", *Phys. Rev. A* **35** (1987) 1802-1808.
17. G. Horvay and J. W. Cahn, "Dendritic and spheroidal growth", *Acta Metall.* **9** (1961) 695-705.
18. G. P. Ivantsov, "Temperature field around a spheroidal, cylindrical and acicular crystal growing in a supercooled melt", *Doklady Akad. Nauk SSSR*, **58** (1947) 567-569 (in Russian). Translated to English and reprinted in Ref. [2], p243-245.
19. P. Pélce and Y. Pomeau, "Dendrites in the small undercooling limit", *Studies in Appl. Math.* **74** (1986) 245-258. See, also: M. Ben Amar, "Theory of needle crystal", *Physica D* **31** (1988) 409-423.
20. R. C. Brower, D. A. Kessler, J. Koplik and H. Levine, "Geometrical approach to moving interface dynamics", *Phys. Rev. Lett.* **51** (1983) 1111-1114.
21. E. Ben-Jacob, N. D. Goldenfeld, J. S. Langer and G. Schön, "Dynamics of interfacial pattern formation" *Phys. Rev. Lett.* **51** (1983) 1930-1932.
22. J. M. Hammersley and G. Mazzarino, "A differential equation connected with the dendritic growth of crystals", *IMA. J. of App. Math.* **42** (1989) 43-75; M. D. Kruskal and H. Segur, "Asymptotics beyond all orders in a model of crystal growth", preprint (1990).
23. D. A. Kessler, J. Koplik and H. Levine, "Steady-state dendritic crystal growth", *Phys. Rev. A* **33** (1986) 3352-3357.
24. B. Caroli, C. Caroli, C. Misbah and B. Roulet, "On velocity selection for needle-crystals in a fully non-local model of solidification", *J. Physique* **48** (1987) 547-551.
25. A. Barbieri and J. S. Langer, "Predictions of dendritic growth rates in the linearized solvability theory", *Phys. Rev. A* **39** (1989) 5314-5325.
26. D. Meiron, "Selection of steady states in the two-dimensional symmetric model of dendritic growth", *Phys. Rev. A* **33** (1986) 2704-2715; M. Ben Amar and B. Moussalam, "Numerical results on two-dimensional dendritic solidification", *Physica D* **25** (1986) 155-164; Y. Saito, G. Goldbeck-Wood and H. Müller-Krumbhaar, "Numerical simulation of dendritic growth", *Phys. Rev. A* **38** (1988) 2148-2157.

27. D. A. Kessler and H. Levine, "Growth velocity of three-dimensional dendritic crystals" *Phys. Rev. A* **36** (1987) 4123-4126.
28. M. N. Barber, A. Barbieri and J. S. Langer, "Dynamics of dendritic sidebranching selection in the two-dimensional symmetric model of solidification", *Phys. Rev. A* **36** (1987) 3340-3349.
29. R. Pieters and J. S. Langer, "Noise-driven sidebranching in the boundary-layer model of dendritic solidification", *Phys. Rev. Lett.* **56** (1986) 1948-1951; R. Pieters, "Noise induced sidebranching in the boundary-layer model of dendritic solidification", *Phys. Rev. A* **37** (1988) 3126-3143.
30. D. A. Kessler and H. Levine, "Determining the wavelength of dendritic sidebranches", *Europhys. Lett.* **4** (1987) 215-221.
31. J. S. Langer, "Dendritic sidebranching in the three-dimensional symmetric model in the presence of noise", *Phys. Rev. A* **36** (1987) 3350-3358.
32. X. W. Qian and H. Z. Cummins, "Dendritic sidebranching initiation by a localized heat pulse", *Phys. Rev. Lett.* **64** (1990) 3038-3041.

Department of Mathematics  
School of Mathematical Science  
Australian National University  
GPO Box 4, Canberra  
ACT-2601, Australia.